FUNCTIONAL NEURORADIOLOGY

Functional magnetic resonance imaging of the human spinal cord during vibration stimulation of different dermatomes

**Jane M. Lawrence · Patrick W. Stroman ·
Spyros S. Kollias**

Abstract

Introduction We investigated noninvasively areas of the healthy human spinal cord that become active in response to vibration stimulation of different dermatomes using functional magnetic resonance imaging (fMRI). The objectives of this study were to: (1) examine the patterns of consistent activity in the spinal cord during vibration stimulation of the skin, and (2) investigate the rostrocaudal distribution of active pixels when stimulation was applied to different dermatomes.

Methods FMRI of the cervical and lumbar spinal cord of seven healthy human subjects was carried out during vibration stimulation of six different dermatomes. In separate experiments, vibratory stimulation (about 50 Hz) was applied to the right biceps, wrist, palm, patella, Achilles tendon and left palm.

Results The segmental distribution of activity observed by fMRI corresponded well with known spinal cord neuroanatomy. The peak number of active pixels was observed at the expected level of the spinal cord with some activity in the adjacent segments. The rostrocaudal distribution of activity was observed to correspond to the dermatome being stimulated. Cross-sectional localization of activity was primarily in dorsal areas but also spread into ventral and intermediate areas of the gray matter and a distinct laterality ipsilateral to the stimulated limb was not observed.

Conclusion We demonstrated that fMRI can detect a dermatome-dependent pattern of spinal cord activity during vibratory stimulation and can be used as a passive stimulus for the noninvasive assessment of the functional integrity of the human spinal cord. Demonstration of cross-sectional selectivity of the activation awaits further methodological and experimental refinements.

Keywords fMRI · Human spinal cord · Vibration · Dermatomes

J. M. Lawrence · S. S. Kollias (✉)
Institute of Neuroradiology, University Hospital of Zurich,
Frauenklinikstrasse 10,
8091 Zurich, Switzerland
e-mail: kollias@dmr.usz.ch

J. M. Lawrence
Department of Physiology, University of Manitoba,
Winnipeg, Manitoba, Canada

P. W. Stroman
Department of Diagnostic Radiology, Queen's University,
Kingston, Ontario, Canada

Introduction

Functional magnetic resonance imaging (fMRI) has been employed to investigate the function of healthy and injured spinal cords in humans during thermal, mechanical, and electrical sensory stimulation and motor tasks [1–6]. These tasks activate an extensive spinal cord network and elicit complicated reflex patterns. In an effort to demonstrate that fMRI can be used noninvasively to localize spinal cord activity, we administered a vibration stimulus to elicit focal neuronal activity.

Vibration stimulation is anticipated to produce more localized patterns of stimuli due to the specificity of sensory recruitment. Vibration stimuli are transduced by two types of mechanoreceptors, Meissner and Pacinian corpuscles that differ in physical and responsive properties. Meissner corpuscles are more sensitive to low-frequency stimulation (5–40 Hz), whereas Pacinian corpuscles are sensitive to higher frequencies (60–300 Hz) [7]. Brain fMRI studies have suggested that Meissner and Pacinian

afferents have different representations at the cortical level [8, 9]. FMRI has not yet been used to investigate areas of spinal cord activity in response to vibration.

Conventional brain fMRI employs a gradient echo imaging sequence that is sensitive to the blood oxygenation level-dependent (BOLD) effect. FMRI in the spinal cord (spinal fMRI) presents unique challenges due to its small cross-sectional dimensions and the magnetically heterogeneous tissues that surround it (cerebrospinal fluid, spinal column, musculature, fat, and lungs). To minimize problems related to the poor field homogeneity, a fast spin-echo sequence with a minimum echo time providing proton-weighted images was used in this present study, as in previous studies [2, 5, 10–12]. This method reveals a second contrast mechanism termed "signal enhancement by extra-vascular water protons" (SEEP) that is an important source of neuronal activity-related signal change in spinal fMRI [10, 12]. The functionally induced signal is theorized to result from neuronal or glial swelling at sites of activity, as well as an increase in localized extravascular water due to the increased intravascular pressure, which accompanies the increased blood flow [13]. Therefore, the signal change is believed to be more localized to sites of neuronal activity than that arising from the BOLD effect. Nonetheless, the signal change observed in the present study would be expected to have contributions from both the BOLD and SEEP effects [10].

In the present study we investigated patterns of neuronal activity detected by spinal fMRI during stimulation of five different dermatomes. Activity was expected in the fifth cervical (C5) spinal cord segment during biceps stimulation, the C7 segment during wrist stimulation, the C8 and first thoracic (T1) segments during palm stimulation, the fourth lumbar (L4) segment during patella stimulation, and the first sacral (S1) segment during Achilles tendon stimulation.

The objectives of this study were twofold. First, we examined the areas of spinal cord that were consistently activated in several subjects during vibration stimulation of the skin. Second, we investigated the rostrocaudal distribution of active pixels during vibration stimulation of different dermatomes. We hypothesized that the areas of signal change would be greatest in the spinal cord segments that innervate the dermatomes stimulated. We also demonstrate that spinal fMRI holds promise as a noninvasive tool for assessment of human spinal cord function.

Materials and methods

Seven healthy volunteers (four male, three female; mean age 28.5±6 years) were imaged using a 1.5-T clinical MR system (Intera, software release 10, Philips Medical Systems,

Best, The Netherlands) positioned supine on a phased array spine coil. Subjects provided written consent prior to scanning. Spinal fMRI data were acquired from seven, 7-mm thick transverse slices aligned alternately with the inter-vertebral discs and the central portions of the vertebral bodies to span a range corresponding to the level at which activity was expected. Vibration stimulation (about 50 Hz) was applied to the biceps, the wrist, the right palm, the patella and the Achilles tendon. In six subjects the left palm was also stimulated (in one subject the left palm was not stimulated due to time restrictions).

During biceps stimulation slices were positioned spanning vertebrae C4 to C7. During wrist and palm stimulation slices were positioned covering vertebrae C6 to T2. During lumbar spinal cord studies the slices were positioned spanning vertebrae T10 to L1. A single shot, fast spin-echo sequence was used with TE 40 ms, TR 6,000 ms, turbo spin echo factor 67, FOV 120 mm, and matrix 128×128 resulting in an in-plane resolution of 0.9×0.9 mm. Flow compensation pulses were applied in the through-slice direction. Saturation pulses were applied to eliminate signal from surrounding regions, and to reduce motion artefacts from breathing and swallowing. A stimulation paradigm consisting of seven alternating rest and stimulation conditions with eight volumes acquired during each block was used (total of 56 volumes).

Data were analyzed based on a general linear model as previously described [2] using custom software written in MatLab (MathWorks, Natick, Mass.). Signal intensity changes were correlated with uncorrected $P \leq 0.05$ to a defined model of the block paradigm of vibration stimulation. Individual maps revealed pixels in which signal change correlated with the defined paradigm and so were considered "active" pixels. The rostrocaudal distribution of activity was assessed quantitatively by counting the number of active pixels in each slice. Time courses of percentage signal change were calculated for all active pixels in all seven slices for each subject. The mean time course was calculated to determine the average time course for the group.

Combined activity maps were created as previously described [2]. Each slice of the individual activity maps was overlaid and manually aligned onto a corresponding anatomical reference image of the same slice and then summed. In-plane smoothing was applied to consider each active pixel's nearest neighbour (one pixel in every direction) to account for imperfect alignment. A threshold of three was then applied to set the minimum number of times a given pixel had to be observed to be active in the individual activity maps in order for it to appear active in the combined activity map. As a result active pixels had to be seen in at least three of the seven maps to appear active in the combined activation map. A colour scale was applied

with yellow indicating pixels at threshold and greater overlap indicated by increasing spectral order.

All applicable institutional and government regulations concerning the ethical use of human volunteers were followed during the course of this research.

Results

A plot of the average number of active pixels observed in each slice is shown in Fig. 1. During biceps stimulation activity was observed bilaterally in the ventral horns at the C5 vertebral level, and in the right dorsal horn at the level of the C5/C6 disc (Fig. 2a). Smaller clusters of active pixels were near the central canal and in the left dorsal horn at the C6 vertebral level and in the right dorsal horn at the level of the C6/C7 disc. The peak signal change was approximately 7% (Fig. 2b), consistent with previously reported signal changes [14].

During wrist stimulation active pixels were observed in the right dorsal horn at the level of the C6/C7 disc, in the left dorsal horn at the level of the C7 vertebra, and bilaterally in the ventral horns at the level of the T1 vertebra (Fig. 3a).

Peak signal changes in these areas were between 7% and 8% (Fig. 3d).

During right and left palm stimulation (Fig. 3b,c), active pixels were mainly at the levels of the C6/C7 disc and C7 vertebra. Within these slices, a larger spread of activity was seen during right palm stimulation; however, data for the right palm were collected from seven subjects, and for the left palm from only six subjects. During right palm stimulation active pixels at the level of the C6/C7 disc were in the left dorsal horn, while those at the C7 vertebra were in the right and left ventral horns. During left palm stimulation, activity was observed in the right dorsal horn of the C6/C7 disc and in the intermediate zone at the C7 vertebra. Peak signal changes of both average time courses were between 6% and 9% (Fig. 3e,f).

Vibratory stimulation of the patella elicited activity in the right dorsal horn at the level of the T11 vertebra and in the left dorsal horn at the level of the T11/T12 disc (Fig. 4a). A small amount of activity was also observed in the left ventral horn at this level. At the level of the T12 vertebra some activity was seen at the edge of the intermediate zone. Peak signal changes of the average time course were between 4% and 7% (Fig. 4c).
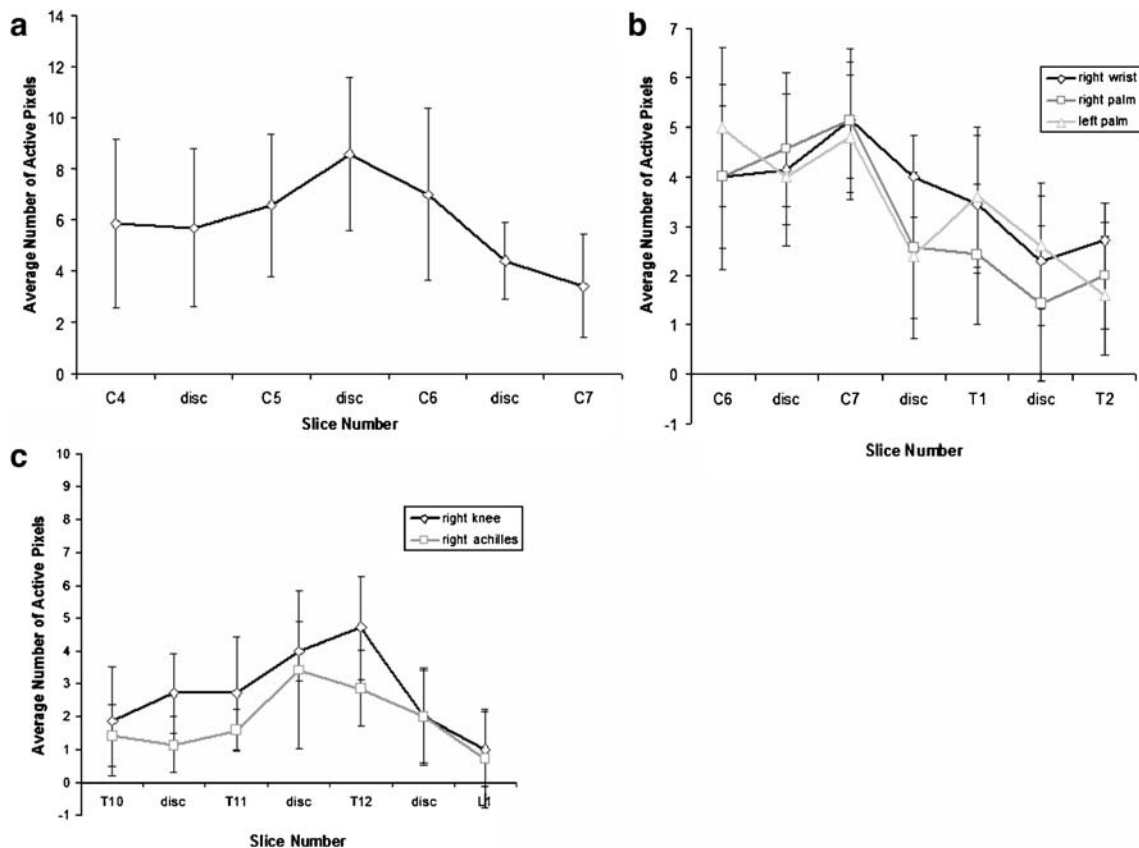

Fig. 1 Average numbers of activated pixels observed with stimulation of (**a**) the right biceps, (**b**) the right wrist and left and right palm, and (**c**) the right knee and Achilles tendon. Error bars indicate the standard error between subjects

Fig. 2 Right biceps stimulation.
a Combined activation map
from seven subjects. Images are
in radiological orientation with
the right side of the body on the
left side of the image and the
dorsal side toward the bottom.
Areas of activity are thresholded
so that a pixel must appear
active at least three times.
b Average time course of a. The
dashed line indicates the
modelled time course
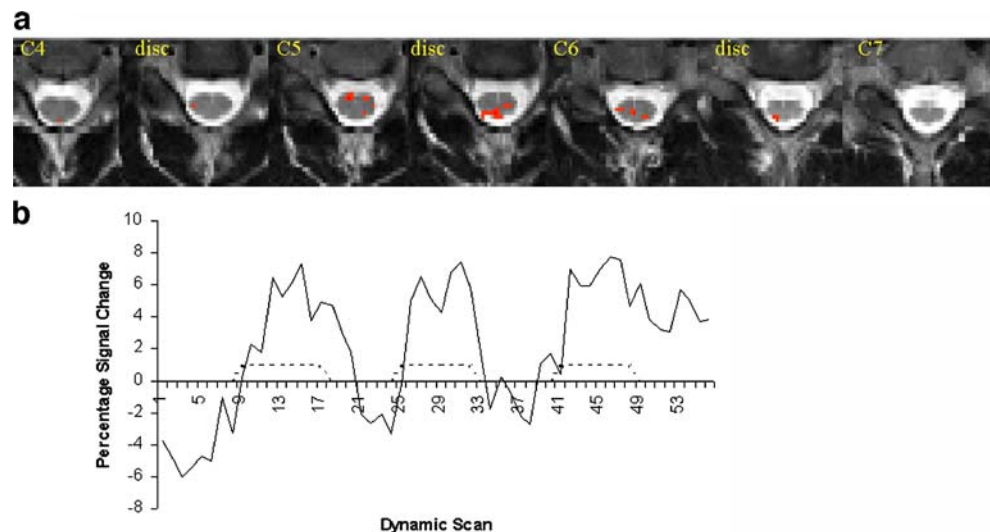
Vibratory stimulation of the Achilles tendon resulted in activity mainly in the ventral horns, but at the T11/T12 disc level activity was also seen in the intermediate zone (Fig. 4b). Dorsal horn activity was observed at the level of the T10 vertebra and the T12/L1 disc. Peak signal changes were between 4% and 7% (Fig. 4d).

Single activity maps from one subject showed a rostro-caudal distribution of active pixels within the expected slices (Fig. 5). During biceps stimulation (Fig. 5a) active pixels were mainly in the right dorsal horn and intermediate zone at the level of the C5/C6 disc. Some active pixels were

also observed in the left dorsal and ventral horn. Wrist stimulation (Fig. 5b) elicited activity slightly more caudal than anticipated at the level of the T1 vertebra, in the dorsal horn bilaterally and the intermediate zone. Only a small number of active pixels were present in the slices caudal to the T1 vertebra. A larger number of active pixels were observed rostral to T1 including the dorsal horns bilaterally at the C6/C7 disc, where activity was anticipated and the ventral horns at the C7 vertebra and the C7/T1 disc (Fig. 5b). During both right and left palm stimulation the greatest number of active pixels were at the level of

Fig. 3 Wrist and palm stimula-
tion. a, b Combined activation
map from seven subjects during
right (a) wrist and (b) palm
stimulation. c Combined activa-
tion maps from six subjects
during left palm stimulation.
Images are in radiological
orientation with the right side of
the body on the left side of the
image and the dorsal side
toward the bottom. Areas of
activity are thresholded so that a
pixel must appear active at least
three times. d–f Average time
courses of the combined maps
shown in a, b and c, respec-
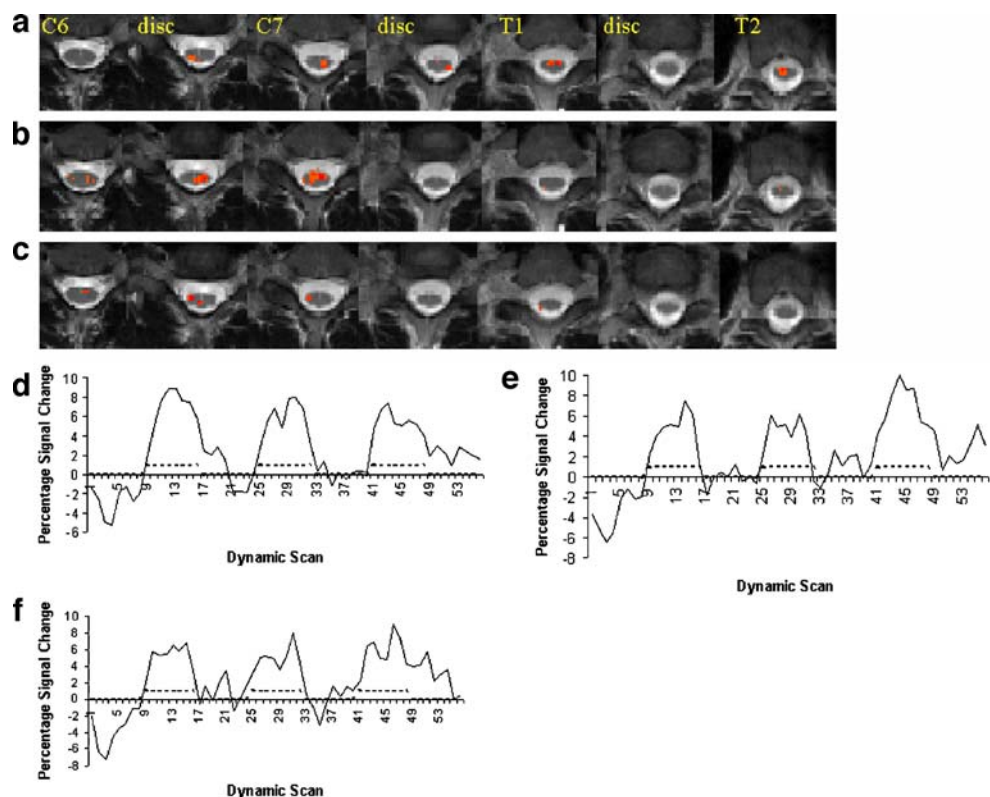tively. The dashed line indicates
the modelled time course

Fig. 4 Knee and Achilles tendon stimulation. **a**, **b** Combined activation map from seven subjects during right (**a**) knee and (**b**) Achilles tendon stimulation. Images are in radiological orientation with the right side of the body on the left side of the image and the dorsal side toward the bottom. Areas of activity are thresholded so that a pixel must appear active at least three times. **c**, **d** Average time courses of the combined maps shown in **a** and **b**, respectively. The dashed line indicates the modelled time course
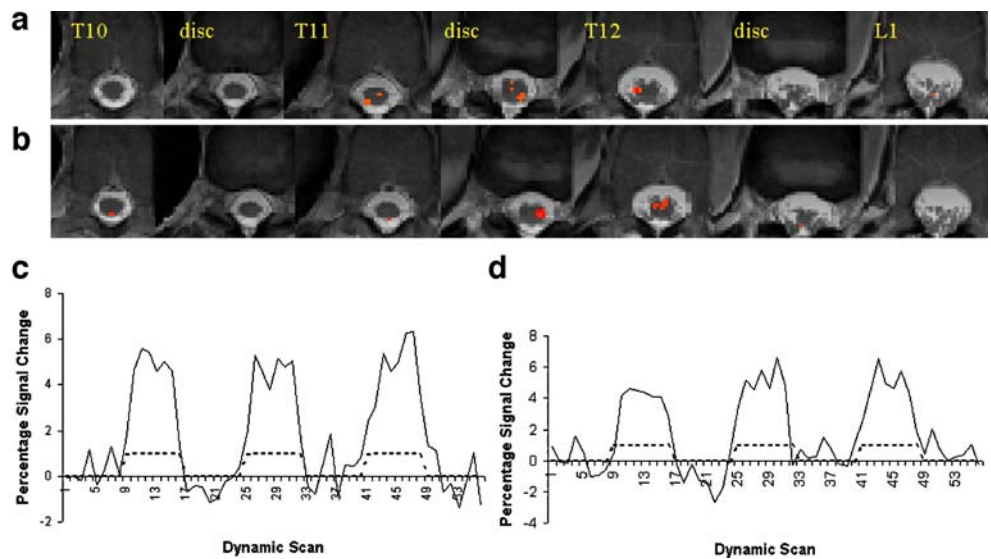
the C7/T1 disc, most often in the dorsal horns bilaterally (Fig. 5c and d, respectively). During both experiments active pixels were most often observed bilaterally in the dorsal horns. Patella stimulation elicited the greatest number of active pixels at the anticipated level, the T11 vertebra

(Fig. 5e). Within this slice several pixels were observed in the dorsal horns bilaterally. Smaller numbers of active pixels were seen in the ventral horns of the adjacent slices. Stimulation of the Achilles tendon resulted in activity in the expected regions at the T11/T12 disc and the level of the

Fig. 5 Activation maps from one subject during stimulation of (**a**) the right biceps, (**b**) the right wrist, (**c**) the right palm, (**d**) the left palm, (**e**) the right patella, and (**f**) the right Achilles tendon. The bars under the images indicate the slices in which peak activity was expected. Images are in radiological orientation with the right side of the body on the left side of the image and the dorsal side toward the bottom
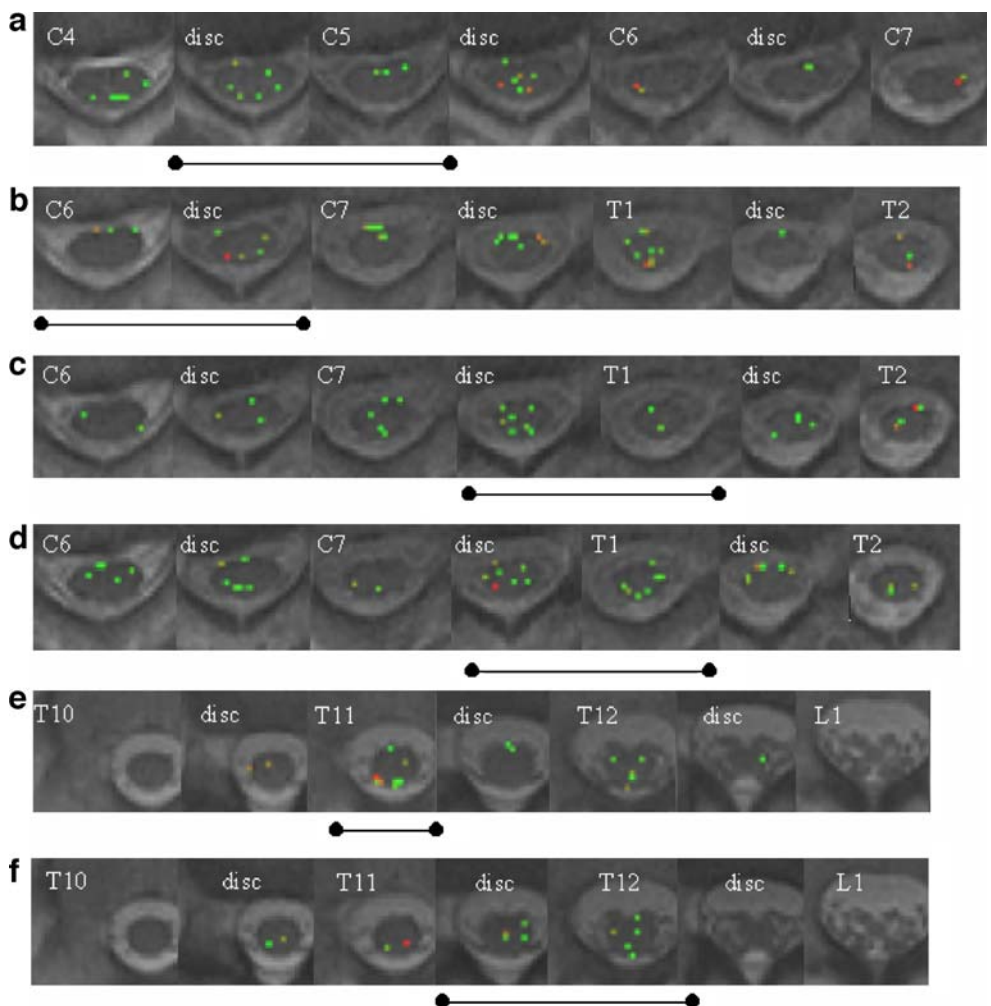
T12 vertebra (Fig. 5f). Two active pixels were present in the slices placed at the T10/T11 disc and the T11 vertebra.

Discussion

Vibration was anticipated to produce more focal activity than previously employed tasks as it recruits Aβ fibres that terminate within laminae III and IV of the dorsal horn [15]. Therefore, active pixels were anticipated in the ipsilateral dorsal horn of the dermatome-specific spinal cord segments. The application of vibration stimulation to different dermatomes did reveal distinct rostrocaudal distributions of activity that corresponded to the appropriate spinal cord levels. Previously, spinal fMRI has been used to examine the rostrocaudal distribution of spinal cord activity during cold thermal stimulation applied to the dermatomes of the little finger, thumb and forearm [14]. The present study confirms that fMRI can be used to detect the appropriate segmental organization in the spinal cord.

As it refers to the cross-sectional localization of activity however, other areas than the ipsilateral dorsal horns were also activated and a distinct laterality ipsilateral to the stimulated limb was not observed. Active pixels were present in both the expected dorsal areas of the gray matter and also ventral and intermediate areas of the gray matter. Physiological and also methodological reasons may be responsible for the spatially distributed pattern of activation within the same or adjacent spinal cord segments. Afferent fibres innervating Pacinian corpuscles, muscle spindles, and tactile receptors make synaptic connections with dorsal horn neurons that project rostrally through the dorsolateral funiculus (DLF) and terminate in the lateral cervical nucleus (LCN) at spinal cord segments C1 and C2. Fibres from the LCN eventually project across the midline and ascend into the medulla where they join the medial lemniscus, which ascends to the ventral posterior lateral (VPL) thalamic nucleus. Eventually, thalamocortical fibres from the VPL project to the primary somatosensory cortex of the postcentral gyrus. According to this organization of central pathways mediating vibration sense a clear lateralization of activity in the ipsilateral dorsal columns should be observed. However, some afferent fibres innervating tactile receptors bifurcate in the dorsal horn, with one branch entering the dorsal columns and the other making a synaptic connection on dorsal horn neurons with axons that cross the midline and project through the lateral spinothalamic tract or the DLF [16]. This early bifurcation and crossing over of afferent fibres in the dorsal horn is the most plausible explanation for the extent of activity in other areas of the spinal cord gray matter and the lack of a clear laterality ipsilateral to the stimulated limb. Moreover, we

also need to emphasize that spinal interneurons receiving cutaneous and proprioceptive input seem to be widely distributed among Rexed's laminas [15]. Given the simultaneous activation of proprioceptive and tactile fibres during vibration stimulation, it would be expected that activity is widespread in both the dorsal and ventral horns as well as intermediate areas of the spinal cord.

Despite the clear segmental distribution of spinal cord activity seen in our study, activity was also present in adjacent segments. The spinal cord is an important site of convergence and divergence of signalling pathways and areas of signal changes were expected to spread over several spinal cord segments. Also the known branching of afferent fibres and the reach network of collateral fibres extending both rostrally and caudally in the spinal cord are likely contributors to the craniocaudal spread of activity. A caveat in this study, as in every study employing axial fMRI acquisition, is that data were collected from spinal cord segments "expected" to show activity according to the stimulated dermatomes and only nearly neighbouring spinal segments were additionally included due to limitations in the temporal resolution of the acquisition. Hence, it is hardly possible to observe a superordinate pattern of rostrocaudally distributed activity that may be physiologically expected from the nature of the applied stimulus. On the other hand, axial acquisitions are preferred for better demonstration of the cross-sectional distribution of activity within the specific segments.

Methodological reasons may also have contributed to the spread of activation in different areas of the spinal cord outside the expected dorsal column ipsilateral to the stimulated body part. Signal changes on both spinal and brain fMRI rely on haemodynamics, and the spatial relationship between the haemodynamic epiphenomena detected with this method and the actual location of neuronal activity remains an open issue. Particularly in spinal fMRI, due to the small cross-sectional dimension of the neural tissue and its specific vascularization pattern, the location of the activated pixels should be evaluated carefully in relation to their proximity to superficial vessels. Often active pixels in the ventral horn were observed at the lateral edge near the position of blood vessels running at the surface of the cord. A previous study has shown that false-positive results can be reduced by identifying and eliminating the contributions from cardiac and respiratory motion [17], but these methods were not employed in the present study. In a more recent study, a high-resolution echo planar imaging stimulation sequence was combined with a sensitivity encoding technique that enhanced the BOLD sensitivity and reduced the signal dropout as well as the image distortions caused by different magnetic susceptibilities in tissues adjacent to the spinal cord [18]. Thus, the authors were able to provide compelling evidence regarding the lateralization and modu-

lation of the spinal neuronal activity as a function of different movement characteristics.

The overlapping of dermatomes and individual variations at the dermatomal boundaries may also account for the less consistent areas of activity observed outside the expected spinal cord segments for the dermatome being stimulated. Care was taken to place the vibrating pad at the same location on each subject. However, due to the size of the pad, more than one dermatome is likely to have been stimulated. During imaging, anatomical land-marking is performed by positioning the imaging slices on the centre of the vertebral bodies and on the intervertebral discs. Intersubject variations in this alignment may have led to an offset in the observed activity in comparison to the expected location. These sources of error may account for the occurrence of active pixels outside the expected segment of the spinal cord and for slight discordances in the location between expected and observed activity.

The use of spinal fMRI to observe neuronal activity noninvasively has obvious clinical advantages. In spinal cord injury and disease, changes in descending modulation and neuroplasticity occur that result in a deviation in the pattern of neuronal activity from normal function. There are currently no adequate, noninvasive clinical imaging methods for the evaluation of spinal cord function. This information could complement electrophysiology testing and disability scores to provide useful prognostic markers related to retained and recovered spinal cord function. Currently, conclusive information regarding stable patterns of neuronal activity cannot be obtained from functional activity maps of individual subjects as these are heavily influenced by transient factors such as physiological noise, descending modulation and sensitivity. As a result, several experiments are needed in order to fully characterize an individual subject's response. In order for spinal fMRI to enter the clinic, further work is needed to optimize scanning and analysis methods to allow an effect evaluation of spinal cord function in individual subjects reproducibly and within an acceptable examination time.

The present study adds to the growing body of literature on spinal fMRI by mapping the regions of spinal cord activity elicited by vibration stimulation. We expand the repertoire of available stimuli and responses that can be assessed with this methodology. We demonstrate that spinal fMRI is capable of detecting a dermatome-specific rostrocaudal distribution in neuronal activity specific to vibration stimulation. At a cross-sectional level, increases in spinal activity were widespread in the dorsal, intermediate and ventral areas of the gray matter, which may reflect the complexity of the reach neuronal connections of the spinal cord but also potential confounding effects of physiological noise. Methodological refinements and future imaging studies will address this issue for further characterization

of the observed activity maps that reflect the organization of central pathways mediating vibration sense. These advances promise to provide a precise and noninvasive method that can be used to obtain novel and quantitative physiological information on the activity of spinal circuits and can be used for the assessment of spinal cord function in the presence of spinal cord pathologies.

References

1. Stroman PW, Kornelsen J, Bergman A, Krause V, Ethans K, Malisza KL, Tomanek B (2004) Noninvasive assessment of the injured human spinal cord by means of functional magnetic resonance imaging. Spinal Cord 42:59–66
2. Kornelsen J, Stroman PW (2004) fMRI of the lumbar spinal cord during a lower limb motor task. Magn Reson Med 52:411–414
3. Backes WH, Mess WH, Wilmink JT (2001) Functional MR imaging of the cervical spinal cord by use of median nerve stimulation and fist clenching. AJNR Am J Neuroradiol 22:1854–1859
4. Kornelsen J, Stroman PW (2007) Detection of the neuronal activity occurring caudal to the site of spinal cord injury that is elicited during lower limb movement tasks. Spinal Cord 45:485–490
5. Ng MC, Wong KK, Li G, Lai S, Yang ES, Hu Y, Luk KD (2006) Proton-density-weighted spinal fMRI with sensorimotor stimulation at 0.2 T. Neuroimage 29:995–999
6. Stracke CP, Pettersson LG, Schoth F, Moller-Hartmann W, Krings T (2005) Interneuronal systems of the cervical spinal cord assessed with BOLD imaging at 1.5 T. Neuroradiology 47:127–133
7. Talbot WH, Darian-Smith I, Kornhuber HH, Mountcastle VB (1968) The sense of flutter-vibration: comparison of the human capacity with response patterns of mechanoreceptive afferents from the monkey hand. J Neurophysiol 31:301–334
8. Harrington GS, Hunter DJ III (2001) FMRI mapping of the somatosensory cortex with vibratory stimuli. Is there a dependency on stimulus frequency? Brain Res 897:188–192
9. Tuunanen PI, Kavec M, Jousmaki V, Usenius JP, Hari R, Salmelin R, Kauppinen RA (2003) Comparison of BOLD fMRI and MEG characteristics to vibrotactile stimulation. Neuroimage 19:1778–1786
10. Stroman PW, Krause V, Malisza KL, Frankenstein UN, Tomanek B (2002) Extravascular proton-density changes as a non-BOLD component of contrast in fMRI of the human spinal cord. Magn Reson Med 48:122–127
11. Li G, Ng MC, Wong KK, Luk KD, Yang ES (2005) Spinal effects of acupuncture stimulation assessed by proton density-weighted functional magnetic resonance imaging at 0.2 T. Magn Reson Imaging 23:995–999
12. Stroman PW, Kornelsen J, Lawrence J, Malisza KL (2005) Functional magnetic resonance imaging based on SEEP contrast: response function and anatomical specificity. Magn Reson Imaging 23:843–850

13. Stroman PW (2005) Magnetic resonance imaging of neuronal function in the spinal cord: spinal FMRI. Clin Med Res 3:146–156

14. Stroman PW, Krause V, Malisza KL, Frankenstein UN, Tomanek B (2002) Functional magnetic resonance imaging of the human cervical spinal cord with stimulation of different sensory dermatomes. Magn Reson Imaging 20:1–6

15. Willis WD, Coggeshall RE (2004) Sensory mechanisms of the spinal cord. Ascending sensory tracts and their descending control. Kluwer Academic/Plenum Publishers, New York, p 292

16. Gilman S (2002) Joint position sense and vibration sense: anatomical organization and assessment. J Neurol Neurosurg Psychiatry 73:473–477

17. Stroman PW (2006) Discrimination of errors from neuronal activity in functional MRI of the human spinal cord by means of general linear model analysis. Magn Reson Med 56:452–456

18. Maieron M, Iannetti GD, Bodurka J, Tracey I, Bandettini PA, Porro CA (2007) Functional responses in the human spinal cord during willed motor actions: evidence for side- and rate-dependent activity. J Neurosci 27:4182–4190